IEEE Access
Multidisciplinary | Rapid Review | Open Access Journal

Received 6 September 2022, accepted 2 October 2022, date of publication 10 October 2022, date of current version 17 October 2022.

Digital Object Identifier 10.1109/ACCESS.2022.3213272

RESEARCH ARTICLE

Modeling of Photovoltaic Inverter Losses for Reactive Power Provision

ROBIN GRAB[1], FRANZISKA HANS[1], MARIANO IVAN ROJAS FLORES[2], HERIBERT SCHMIDT[1], SOENKE ROGALLA[1], AND BERND ENGEL[3], (Member, IEEE)

[1]Fraunhofer Institute for Solar Energy Systems, 79110 Freiburg, Germany
[2]Techint Engineering and Construction S.A., San Luis 5700, Argentina
[3]elenia Institute for High Voltage Technology and Power Systems, Technische Universität Braunschweig, 38106 Brunswick, Germany

Corresponding author: Robin Grab (robin.grab@ise.fraunhofer.de)

This work was supported by the German Ministry for Economic Affairs and Energy under Grant FKZ 0350061B.

ABSTRACT In addition to their main functionality of converting DC input power to AC output power, today's photovoltaic inverters are generally required to be capable of providing reactive power. While there are well-established mathematical models that use the correlation between inverter losses and the transmitted active power to estimate inverter efficiency for any given active power operating point, the additional losses in the inverter due to the supply of reactive power are less well studied. In this work, the conversion efficiencies of three different photovoltaic inverters were measured for various active power and reactive power setpoints. Based on these measurements, two mathematical models are proposed to represent the conversion losses as a function of active and reactive output power. One model is of empirical nature and expands preexisting models to include terms that take the reactive power into consideration. The other model takes the dominant loss mechanisms in the conversion stage of inverters into account and considers the effect of reactive power provision on them. Both models were compared with a model variant proposed in literature. They are shown to perform with high accuracy over the entire operating range, while requiring only a small number of known efficiency values for parametrization. There are several fields of application for these new models: They allow photovoltaic park operators to precisely estimate the individual losses of a solar power plant that feeds reactive power into the grid. For grid operators, they enable a comparative loss analysis for different reactive power sources.

INDEX TERMS DC-AC power converters, loss measurement, photovoltaic systems, power conversion, reactive power control.

I. INTRODUCTION

Due to the global energy transition, more and more renewable energy sources are used to cover the electricity demand. Over the last years, the development of power electronics has enabled solar and wind power plants to contribute to the grid voltage stability with reactive power provision [1], [2]. As a consequence, more and more regulatory bodies and system operators require inverters to deliver reactive power to the grid. Furthermore, recent academic studies (e.g. [3] and [4]) propose to increase the contribution of distributed generation plants (including PV inverters) to the reactive power management of electricity grids to counterbalance the anticipated decommissioning of thermal power plants. Therefore, the consequences of increased reactive power infeed from PV inverters are of greater interest.

PV inverter datasheets generally contain information about peak efficiency and additionally single-figure efficiency metrics like European or CEC efficiency (see for example [5] and [6]). These indications are useful for a first comparison between inverters. However, for a detailed yield analysis, the inverter losses for all relevant operating points need to be considered. Inverter efficiency models can be used for this purpose. These models are parametrized with a limited number of known efficiency values and are designed to calculate inverter efficiencies for any operating point with high accuracy.

The associate editor coordinating the review of this manuscript and approving it for publication was Chi-Seng Lam.

A well-established model to represent the relationship between the efficiency of an inverter and the transmitted active power is the Schmidt-Sauer efficiency model [7], [8]. However, active power output is not the only variable to affect inverter efficiency. In [9], the Schmidt-Sauer model was extended to include the influence of DC voltage on efficiency. Due to the growing role of the provision of auxiliary grid services with PV inverters, it is desirable to develop similar models that take the effects of reactive power infeed into account.

It is common knowledge that the conversion efficiency decreases with a non-unity power factor, but the extent of the additional inverter losses due to the supplied reactive power is less well studied. A few research papers have performed loss analyses for selected inverter topologies [10], [11], yet do not suggest a generalization from their results leading to the formulation of a loss model. In [12] and [13], an approach for a model linking apparent power output and inverter efficiency that is based on the Schmidt-Sauer model is presented. This model can be referred to as ''Braun's model''. While it delivers loss values for any apparent power operating point, it assumes that there is no further influence of the power factor on the power dissipation, yet only supports this assumption with measurement data from two distinct inverters. Nevertheless, Braun's model was used to quantify inverter losses in recent power network studies [14], [15].

In an earlier attempt published in [16], the authors of this study followed a numeric approach and postulated two models called ''Quadratic Approximation Model'' and ''Potential Approximation Model''. However, these models need a large number of known efficiency values for parametrization, which limits their practical use. Moreover, due to their numeric nature, the universality of this approach could not be ensured.

The aim of the present work was to develop a high-accuracy, yet simple-to-use mathematical model for inverter losses at reactive and active power operating points that can be applied to different PV inverter types. Furthermore, the new model should avoid Braun's neglection of the power factor-induced inverter losses.

This manuscript describes the development of the models as well as instructions for their parametrization and application. In Section II, the working principles of the original Schmidt-Sauer model and Braun's model are explained. As data basis for the development of the new models, one central PV inverter and two multi-string inverters were measured at the Fraunhofer Institute for Solar Energy Systems ISE in Freiburg, Germany (Section III). The conversion efficiency of each inverter was evaluated at various operating points consisting of different active and reactive power setpoints. This data was used for model development. Since two distinct approaches were found that have different potential fields of application, both models are presented in this manuscript (Sections IV and V). The models represent the power dissipation of an inverter as a function of both active and reactive output power. They can be parametrized with known conversion efficiency values for a limited number of operating points. Section VI explains how the two new models were evaluated in terms of their accuracy for the entire operating range by comparing the measured efficiency values with the values predicted by the models. The same was done with Braun's model, which allowed for a direct comparison of the three models for each inverter. Finally, Section VII discusses the different areas of application of the individual models and points out their advantages and limitations.

II. SCHMIDT-SAUER MODEL AND BRAUN'S MODEL

The so-called Schmidt-Sauer efficiency model provides a general representation of an inverter's efficiency in relation to the supplied active power.

The efficiency η of any device is defined as the output power P_{out} divided by the input power P_{in}. Since the power dissipation P_{loss} within the device is the difference between input and output power, η can be expressed as a function of P_{out} and P_{loss}, as presented in (1).

$$\eta = \frac{P_{\text{out}}}{P_{\text{in}}} = \frac{P_{\text{out}}}{P_{\text{out}}+P_{\text{loss}}} \tag{1}$$

The physical modeling to describe the efficiency characteristic of an inverter was first developed in 1989 [17] and is based on the assumption that the inverter losses P_{loss} can be represented with a quadratic equation, as shown in (2).

$$P_{\text{loss}} = p_{\text{self}} + v_{\text{loss}} \cdot P_{\text{out}} + r_{\text{loss}} \cdot P_{\text{out}}^2 \tag{2}$$

The so-called Schmidt-Sauer parameters p_{self}, v_{loss} and r_{loss} defining the quadratic equation can be interpreted as in the following (see [8]):

p_{self}: Internal consumption, independent of the load.

v_{loss}: Voltage losses in diodes and bipolar transistors, leading to power losses proportional to the active output power.

r_{loss}: Ohmic losses (in coils, cables and connectors). These losses increase quadratically with the output power.

Consequently, the Schmidt-Sauer model describes the inverter efficiency curve with the set of parameters (p_{self}; v_{loss}; r_{loss}), as shown in (3).

$$\eta = \frac{P_{\text{out}}}{P_{\text{in}}} = \frac{P_{\text{out}}}{P_{\text{out}}+p_{\text{self}} + v_{\text{loss}}\cdot P_{\text{out}} + r_{\text{loss}}\cdot P_{\text{out}}^2} \tag{3}$$

These parameters can be calculated with three efficiency measurements. For model accuracy, it is preferable to use operating points that are spaced out over the operating range. In [8], efficiency measurements at 10%, 50% and 100% of the nominal output power are proposed. The calculation of the parameters is presented in (4), (5) and (6) for these three power values.

$$p_{\text{self}} = \frac{1}{9}\cdot\frac{1}{\eta_{100}} - \frac{1}{4}\cdot\frac{1}{\eta_{50}} + \frac{5}{36}\cdot\frac{1}{\eta_{10}} \tag{4}$$

$$v_{\text{loss}} = -\frac{4}{3}\cdot\frac{1}{\eta_{100}} + \frac{33}{12}\cdot\frac{1}{\eta_{50}} - \frac{5}{12}\cdot\frac{1}{\eta_{10}} - 1 \tag{5}$$

$$r_{\text{loss}} = \frac{20}{9}\cdot\frac{1}{\eta_{100}} - \frac{5}{2}\cdot\frac{1}{\eta_{50}} + \frac{5}{18}\cdot\frac{1}{\eta_{10}} \tag{6}$$

η_{10}, η_{50}, and η_{10} are the efficiencies of the inverter at 10%, 50% and 100% of the nominal output power.

The curves of efficiency versus active power of all modern inverters show a similar pattern, regardless of their hardware topology. An individual parameter set (p_{self}; v_{loss}; r_{loss}) defining the shape of the curve can be determined for any type of inverter. Moreover, it is applicable to single-stage as well as to multi-stage inverters for a fixed DC voltage to AC voltage ratio. After set-up, the model can be used to predict the efficiency for any active power value. When power values are given in pu and the efficiency values in decimal form, then the method produces efficiency results also in decimal form. If the efficiency is desired as a percentage, it must be multiplied by 100%. Similar relationships can be specified for three arbitrary points with some adjustments in the equations.

Braun's model generalizes the Schmidt-Sauer approach so that it can be used for active as well as reactive power operating points. Braun assumes that inverter losses in the case of a non-unity power factor depend on the absolute value of the current alone. In the case of a constant AC terminal voltage, this assumption leads to a loss equation similar to (2), but where active power is replaced with apparent power S_{out} [12]. The resulting quadratic equation modeling the power dissipation is shown in (7).

$$P_{loss} = p_{self} + v_{loss} \cdot S_{out} + r_{loss} \cdot S_{out}^2 \tag{7}$$

The three parameters (p_{self}; v_{loss}; r_{loss}) defining the equation are identical as in the original Schmidt-Sauer model and can be determined with three standard efficiency measurements with unity power factor. Therefore, equations (4), (5) and (6) state the calculation rules for these parameters for known efficiency values at 10%, 50% and 100% of the nominal output power.

III. EXPERIMENTAL SETUP, MEASUREMENTS AND INTERPOLATION

As a part of this work, measurements of conversion efficiency were performed with three PV inverters for a wide range of operating points. These measurements served as the basis for model creation and parametrization (Sections IV and V) as well as for model validation (Section VI). The measurements took place in the TestLab Power Electronics of the Fraunhofer Institute for Solar Energy Systems ISE in Freiburg, Germany. They were based on the procedure defined in the standard EN50530 [18]. The devices under test comprised one central inverter with a nominal power of 1 MVA and two string inverters of 50 kVA and 36 kVA respectively. Fig. 1 shows the circuit used for the measurements of the two string inverters. The input power supply of the inverter was provided by an equivalent DC source that has integrated the characteristic curve of a PV generator determining the relation between current and voltage.

The AC side of the inverter was connected to an AC grid simulator in order to rule out any negative impact of grid events on measurement accuracy. The input DC source and the AC grid simulator were connected to the medium-voltage

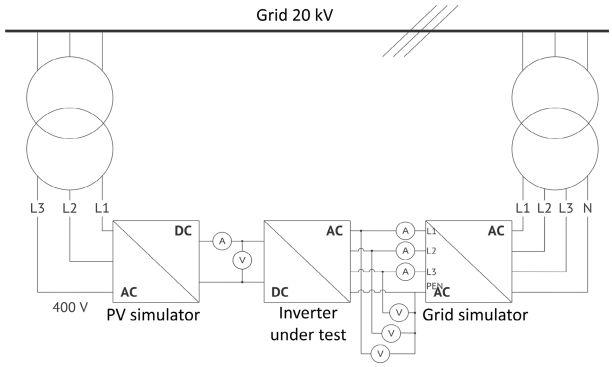

FIGURE 1. Measurement circuit for the two string inverters.

grid via transformers. The DC source was controlled by software to adjust the active power and input voltage to the respective measuring points. The reactive power was controlled by the inverters and was adjusted via their control software.

The 1 MVA central inverter was measured in a comparable setup, the main differences being a direct AC grid connection and the presence of an external auxiliary power supply that was equipped with current and voltage sensors in order to factor in its consumption. These variations in the measurement setup were necessary due to the much larger power of this particular inverter.

In order to get a good data basis for model conception and validation, efficiency values had to be obtained for a large number of points of active and reactive power output (P; Q) over the entire operating range. For all three inverters included in the study, all software restrictions regarding their reactive power range were disabled so that the operating range was limited only by the maximum apparent power on one side and the turn-off limit for very low DC power on the other side. Within this operating range, between 93 and 225 different points were measured for each of the three inverters.

For all measurement points (P; Q), DC input power P_{in} and AC output power P_{out} were recorded and integrated during two-minute measurement periods to obtain the input and output energies from which the conversion efficiency was calculated. In this manner, an average efficiency in integration time T was obtained, as shown in (8).

$$\eta_{\%} = \frac{\int_0^T P_{out} dt}{\int_0^T P_{in} dt} \cdot 100\% \tag{8}$$

For the further modeling steps, it was advantageous to know the efficiency of each inverter not only at the measured points, but also at other power values. Therefore, an interpolation of the measured points (P; Q; η) for round power values was carried out. This interpolation was performed with the "pchip" and the "spline" functions of Matlab [19], [20]. These functions interpolate with third degree polynomials.

In Fig. 2, the measurement data of the 50 kVA string inverter (black dots) are superimposed with the interpolated data represented by the colored area.

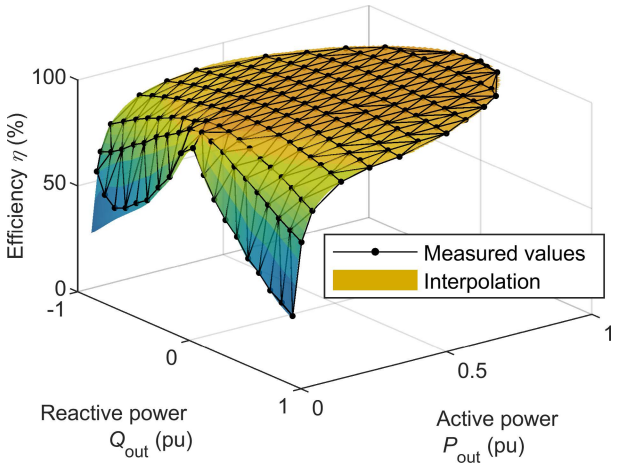

FIGURE 2. Measurement data and interpolated data, 50 kVA inverter.

IV. EMPIRICAL EFFICIENCY MODEL

A. MODEL DEVELOPMENT

The Empirical Efficiency Model (EEM) is based on the observation that for each given reactive power value, the dependence of the losses on the active power output follows the shape of a parabola and can be modeled with a quadratic function (see Fig. 3). Thus, for each reactive power value, an individual set of Schmidt-Sauer parameters (p_{self}; v_{loss}; r_{loss}) can be found. Each parameter is considered as a function of the reactive power Q_{out}, as defined in (9).

$$P_{\text{loss}} = p_{\text{self}}(Q_{\text{out}}) + v_{\text{loss}}(Q_{\text{out}}) \cdot P_{\text{out}} + r_{\text{loss}}(Q_{\text{out}}) \cdot P_{\text{out}}^2 \tag{9}$$

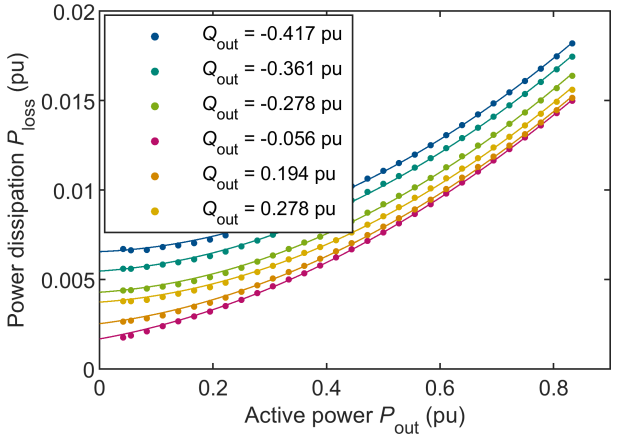

FIGURE 3. Power losses against active power for different reactive power values with compensation parabola, 36 kVA inverter.

With the available measurement data, the relation between each of the three parameters and the reactive power output could be established (Fig. 4). For all three inverters, these curves also roughly follow parabolic courses.

It is therefore possible to describe these parameters with good accuracy with second degree polynomials, as described in (10), (11) and (12).

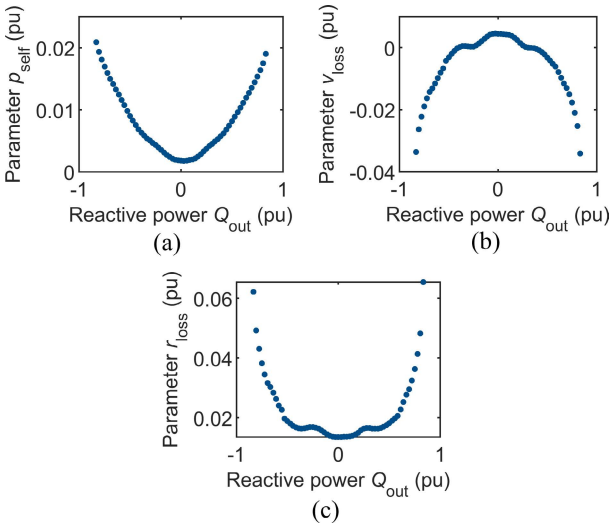

FIGURE 4. Parameters p_{self} (a), v_{loss} (b) and r_{loss} (c) against reactive power, 36 kVA inverter.

$$p_{\text{self}}(Q_{\text{out}}) = p_{\text{self},0} + p_{\text{self},1} \cdot Q_{\text{out}} + p_{\text{self},2} \cdot Q_{\text{out}}^2 \tag{10}$$

$$v_{\text{loss}}(Q_{\text{out}}) = v_{\text{loss},0} + v_{\text{loss},1} \cdot Q_{\text{out}} + v_{\text{loss},2} \cdot Q_{\text{out}}^2 \tag{11}$$

$$r_{\text{loss}}(Q_{\text{out}}) = r_{\text{loss},0} + r_{\text{loss},1} \cdot Q_{\text{out}} + r_{\text{loss},2} \cdot Q_{\text{out}}^2 \tag{12}$$

Incidentally, this approach resembles established models that describe the dependence of inverter losses on DC voltage and active power [9], [21].

The EEM is thus defined on the basis of nine independent parameters. Three of them ($p_{\text{self},0}$; $v_{\text{loss},0}$; $r_{\text{loss},0}$) correspond to the Schmidt-Sauer parameters and describe the losses for pure active power injection, whereas the loss behavior for additional reactive power supply is determined by the remaining six parameters ($p_{\text{self},1}$; $v_{\text{loss},1}$; $r_{\text{loss},1}$; $p_{\text{self},2}$; $v_{\text{loss},2}$; $r_{\text{loss},2}$).

B. CALCULATION RULES FOR THE MODEL PARAMETERS

To determine these nine parameters, nine independent efficiency measurements for different points (P; Q) in the operational area have to be performed. The resulting system of equations can be solved for any combination of points. However, it is preferable to use points that are spaced out evenly in order to get good model accuracy in the entire operational area. Moreover, using some points with zero reactive power simplifies the ensuing calculations.

Therefore, the authors propose to use measurement points that comprise the original three Schmidt-Sauer points with zero reactive power as well as six additional points that cover a wide part of the reactive power operational area. For the selection of these six points, it is advantageous to perform the measurements for inductive and capacitive reactive power with symmetrical magnitudes, as this simplifies the measurement process considerably. With these boundary conditions, a set of measurement points was optimized to achieve the lowest average model error for the 50 kW string inverter. Since it also provided high accuracy for the other tested inverters, it is proposed to use these measurement points in general for

the EEM. The set consists of the Schmidt-Sauer points ($\eta_{10;0}$; $\eta_{50;0}$; $\eta_{90;0}$) and the additional points ($\eta_{20;70}$; $\eta_{20;-70}$; $\eta_{50;70}$; $\eta_{50;-70}$; $\eta_{70;70}$; $\eta_{70;-70}$) for both inductive and capacitive reactive power (see Fig. 5). In this representation, the first index stands for the active power value and the second for the reactive power value, both given as a percentage of the nominal power.

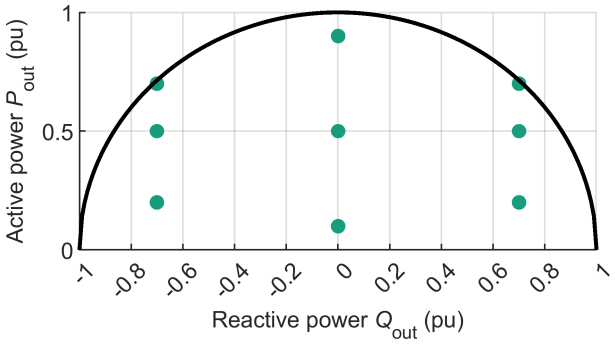

FIGURE 5. Proposed measurement points for the empirical efficiency model.

For this set of measurement points, rules of calculation for the parameters of the EEM can be found by solving the corresponding system of equations. The parameters $p_{\text{self},0}$; $v_{\text{loss},0}$ and $r_{\text{loss},0}$ correspond to the Schmidt-Sauer parameters and can be calculated as shown in (4), (5) and (6). The calculation rules for the remaining six parameters are described in (13). If the use of other measurement points is desired, it is necessary to adjust the calculation rules by setting up and solving the system of equations for these respective points.

$$\begin{bmatrix} p_{self,1} \\ v_{loss,1} \\ r_{loss,1} \\ p_{self,2} \\ v_{loss,2} \\ r_{loss,2} \end{bmatrix} = [M]_{6x6} \cdot \begin{bmatrix} \frac{1}{\eta_{20;70}} \\ \frac{1}{\eta_{20;-70}} \\ \frac{1}{\eta_{50;70}} \\ \frac{1}{\eta_{50;-70}} \\ \frac{1}{\eta_{70;70}} \\ \frac{1}{\eta_{70;-70}} \end{bmatrix} - \frac{100}{49} \cdot \begin{bmatrix} 0 \\ 0 \\ 0 \\ p_{self,0} \\ v_{loss,0}+1 \\ r_{loss0} \end{bmatrix} \tag{13}$$

where

$$M = \begin{bmatrix} \frac{1}{3} & -\frac{1}{3} & -\frac{5}{6} & \frac{5}{6} & \frac{1}{2} & -\frac{1}{2} \\ -\frac{8}{7} & \frac{8}{7} & \frac{75}{14} & -\frac{75}{14} & -\frac{7}{2} & \frac{7}{2} \\ \frac{20}{21} & -\frac{20}{21} & -\frac{125}{21} & \frac{125}{21} & 5 & -5 \\ \frac{10}{21} & \frac{10}{21} & -\frac{25}{21} & -\frac{25}{21} & \frac{5}{7} & \frac{5}{7} \\ -\frac{80}{49} & \frac{80}{49} & \frac{375}{49} & \frac{375}{49} & -5 & -5 \\ \frac{200}{147} & \frac{200}{147} & -\frac{1250}{147} & -\frac{1250}{147} & \frac{50}{7} & \frac{50}{7} \end{bmatrix}$$

In summary, when efficiency values for nine operating points ($\eta_{10;0}$; $\eta_{50;0}$; $\eta_{90;0}$;$\eta_{20;70}$; $\eta_{20;-70}$; $\eta_{50;70}$; $\eta_{50;-70}$; $\eta_{70;70}$;$\eta_{70;-70}$) are known, the model parameters can be determined with the calculation rules given in (4), (5), (6), and (13). Any type of inverter will have an individual set of parameters ($p_{\text{self},0}$; $v_{\text{loss},0}$; $r_{\text{loss},0}$; $p_{\text{self},1}$; $v_{\text{loss},1}$; $r_{\text{loss},1}$; $p_{\text{self},2}$; $v_{\text{loss},2}$; $r_{\text{loss},2}$) describing its efficiency plane versus active and reactive power. By inserting these parameters in (10), (11), (12), and finally (9), inverter losses for any value of active and reactive power can be predicted with the EEM.

V. LOSS-BASED EFFICIENCY MODEL

A. MODEL DEVELOPMENT

In the course of this study, the EEM showed good usability and accuracy for all tested inverters. While it can be assumed that this is true for most inverter types, the general applicability of empirical models cannot be proven. In an attempt to avoid purely empirical methods, an entirely different approach was used that led to the development of a second model, the so-called Loss-Based Efficiency Model (LEM). This model takes the physical effects that cause losses in any kind of PV inverter into account.

There are multiple different effects in the conversion step of an inverter that lead to additional losses when reactive power is supplied. These effects can be categorized in two groups: First, the higher current value due to reactive power supply causes increased losses inside several physical components of the inverter. This is usually the dominating effect and is considered in Braun's model. Second, the altered phase angle may originate additional losses in some elements that participate in the conversion step. This effect is neglected in Braun's approach. By considering the most important loss mechanisms of an inverter one by one, the underlying effect for each mechanism can be determined.

1) LOSS MECHANISMS IN INVERTERS

The power semiconductors (switches and diodes) of an inverter operate in switching mode. Conduction and switching losses have the biggest share of the overall semiconductor losses, while blocking and control losses play a minor role [22] and will be left out for this evaluation.

The total conduction losses of an inverter are the sum of the individual conduction losses P_{cond} of the internal switches and diodes. They are determined by the voltage drop v_{S} across and current flow i_{S} through each semiconductor over a switching period T_{sw} [23], as given in (14).

$$P_{\text{cond}} = \frac{1}{T_{\text{sw}}} \int_0^{T_{\text{sw}}} v_{\text{S}}(t) \cdot i_{\text{S}}(t) dt \tag{14}$$

The forward voltage of a semiconductor v_{S} can be approximated linearly by introducing the threshold voltage V_{S0} and differential resistance r_{d} [24], as shown in (15).

$$v_{\text{S}} = V_{\text{S0}} + r_{\text{d}} \cdot i_{\text{S}} \tag{15}$$

Therefore, the average conduction losses $P_{\text{cond,avg}}$ of a semiconductor [25] can be calculated as presented in (16).

$$P_{\text{cond,avg}} = V_{\text{S0}} \cdot i_{\text{S,avg}} + r_{\text{d}} \cdot i_{\text{S,RMS}}^2 \tag{16}$$

In this equation, $i_{\text{S,avg}}$ and $i_{\text{S,RMS}}$ represent the average magnitude and the RMS value of the forward current through the semiconductor. This relation demonstrates that the conduction losses depend directly on the magnitude of the current. Moreover, the threshold voltage V_{S0} and the differential

resistance r_d of the switches and the diodes are not generally identical. Since the phase angle of the current decides which share is conducted by each semiconductor, the total conduction losses of an inverter also depend on the phase angle of the injected current.

The switching losses $P_{on/off}$ are defined as the product of current and voltage during the switching process [26], as shown in (17).

$$P_{on/off} = f_s \int_0^{t_{on/off}} v_S(t) \cdot i_S(t) dt \tag{17}$$

Therefore, alongside the switching frequency f_s, they depend on the magnitude of the current. Since the current phase angle influences the moment in time when the switching takes place, it also alters the current and voltage values during the switching process and thus the switching losses. Consequently, the switching losses depend on the phase angle as well.

Besides the semiconductors, the filter coils are the second most important elements where losses occur inside an inverter. The main loss mechanisms of the coils are core losses P_{core} and winding losses $P_{winding}$, as shown in (18).

$$P_{coil} = P_{core} + P_{winding} \tag{18}$$

The core losses depend essentially on the magnetic flux density and therefore increase with the current, but do not depend on the phase angle [27], [28]. Winding losses comprise DC conduction losses $P_{winding,DC}$, which are dependent on the absolute value of the current, and AC losses $P_{winding,AC}$ influenced by skin and proximity effects, as given in (19).

$$P_{winding} = P_{winding,DC} + P_{winding,AC} \tag{19}$$

The AC losses depend on the current frequency and the winding geometry, not on the reactive power value. In conclusion, when an inverter feeds in reactive power, the losses in the filter coils vary as a function of the increased current but are not directly influenced by the changing phase angle.

Another important loss mechanism in an inverter is caused by ohmic losses of the internal conducting paths and electrical connections. These losses depend on the magnitude of the current, but not on its phase angle.

Losses in other elements such as capacitors, fuses etc. are marginal [22] and need not be considered in the modeling.

In summary, the changing losses due to reactive power injection can be divided into two groups:

- Losses that are a function of the output current alone and increase due to the larger apparent current
- Losses that are additionally a direct function of the phase angle

Fig. 6 shows a graphical assignment of the main loss mechanisms into the two groups.

2) MODEL ADAPTATION BASED ON LOSSES

Considering these findings, the Schmidt-Sauer model can be adapted accordingly. The increased current can be taken into account by exchanging the active power P_{out} with the apparent power S_{out}. The phase angle dependency of the switching losses is represented by replacing the voltage loss constant v_{loss} with a function v_{loss} (cos φ). Similarly, the ohmic loss function r_{loss} (cos φ) takes into account that the conduction losses of the semiconductors may as well vary with the phase angle. The parameter p_{self} describes the internal losses and is considered to be independent from output power or phase angle and therefore a constant value, just as in the original Schmidt-Sauer model.

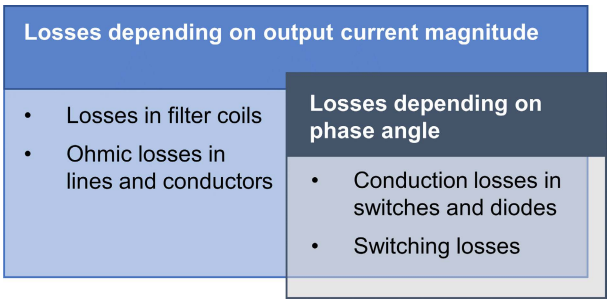

FIGURE 6. Classification of different loss mechanisms during reactive power feed-in of inverters.

The resulting model equation of the LEM is shown in (20).

$$P_{loss} = p_{self} + v_{loss}(\cos\varphi) \cdot S_{out} + r_{loss}(\cos\varphi) \cdot S_{out}^2 \tag{20}$$

Fig. 7 shows a plot of the power dissipation of the 36 kVA inverter against the apparent power for different power factor values cos φ. This figure confirms the definition of p_{self} as a constant that is independent from output power and phase angle. The other parameters describing each compensation parabola vary with cos φ. The figure further confirms that the assumption taken in [12] that inverter losses only depend on apparent power output and not on the power factor are not accurate for this inverter.

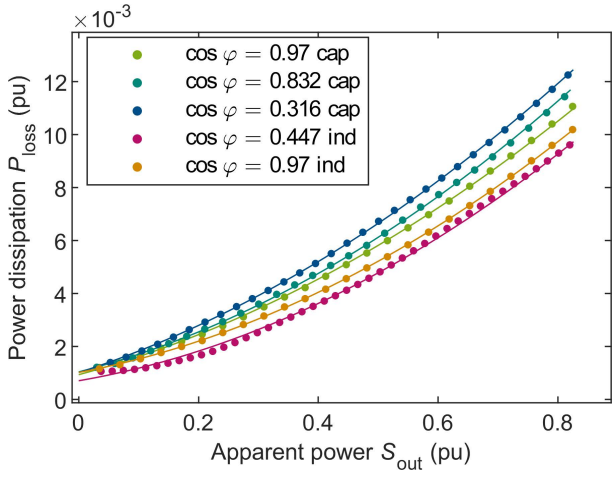

FIGURE 7. Power loss against apparent power for different power factor values with compensation parabola, 36 kVA inverter.

The relation between cos φ and the parabola coefficients v_{loss} and r_{loss} for this inverter are shown in Fig. 8.

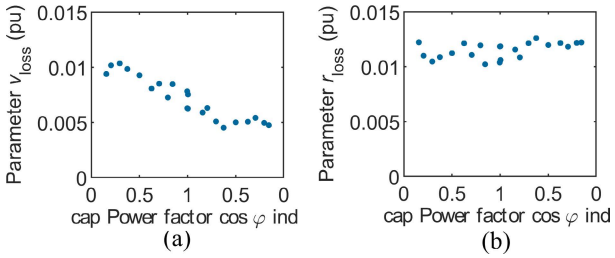

FIGURE 8. Loss parameters v_{loss} (a) and r_{loss} (b) against power factor cos φ, 36 kVA inverter.

Simple linear equations were chosen to approximate the loss parameter functions v_{loss} (cos φ) and r_{loss} (cos φ), as shown in (21) and (22).

$$v_{loss}(\cos\varphi) = v_{loss,a} + v_{loss,b} \cdot \cos\varphi \tag{21}$$

$$r_{loss}(\cos\varphi) = r_{loss,a} + r_{loss,b} \cdot \cos\varphi \tag{22}$$

The LEM is thus defined on the basis of five independent parameters (p_{self}; $v_{loss,a}$; $r_{loss,a}$; $v_{loss,b}$; $r_{loss,b}$).

The constant parameter p_{self} is interpreted as the self-consumption of the inverter. The parameters $v_{loss,a}$ and $v_{loss,b}$ describe the voltage losses that increase proportionally to the output current and thus to the output apparent power. The voltage losses have one component $v_{loss,a}$ that is independent of the power factor and another component $v_{loss,b}$ that defines the influence of the power factor. Analogously, the parameters $r_{loss,a}$ and $r_{loss,b}$ define the ohmic losses.

B. CALCULATION RULES FOR THE MODEL PARAMETERS

In order to determine these five parameters, five independent efficiency measurements for different points (S; cos φ) in the operational area have to be performed. The resulting system of equations can be solved for any combination of points. However, it is again preferable to use points that are spaced out in order to achieve good model accuracy in the entire operational area. Moreover, using some points with a power factor of one simplifies the ensuing calculations. It is proposed to use the three original Schmidt-Sauer points ($\eta_{10;1}$; $\eta_{50;1}$; $\eta_{90;1}$). In this representation, the first index stands for the active power value given as a percentage of the nominal power, while the second index describes the point's power factor.

The calculations become simpler when the remaining two measurement points have the same power factor. It was found that with these boundary conditions, the lowest average model error for the 50 kVA string inverter was reached for the measurement points $\eta_{50;0.6}$ and $\eta_{100;0.6}$. Since it also showed high accuracy for the other tested inverters, it is proposed to use these measurement points in general for the LEM. Fig. 9 shows the position of the proposed measurement points in the operational area.

For this set of measurement points, rules of calculation for the parameters of the LEM can be found by solving the corresponding system of equations. The parameter p_{self} can be determined as shown in (4). It is also required to calculate the two other Schmidt-Sauer parameters v_{loss} and r_{loss} as

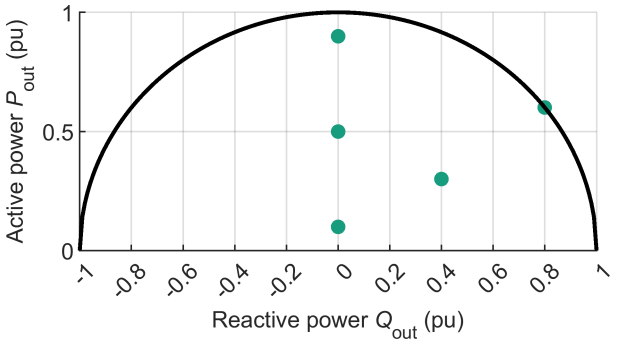

FIGURE 9. Proposed measurement points for the loss-based efficiency model.

described in (5) and (6) as an intermediate step. With this, $v_{loss,b}$ and $r_{loss,b}$ can be calculated with the equations shown in (23) and (24).

$$v_{loss,b} = \frac{15}{2}\cdot p_{self} + \frac{5}{2}\cdot v_{loss} - 3\cdot\frac{1}{\eta_{50;0.6}} + \frac{3}{2}\cdot\frac{1}{\eta_{100;0.6}} + \frac{3}{2} \tag{23}$$

$$r_{loss,b} = -5\cdot p_{self} + \frac{5}{2}\cdot r_{loss} + 3\cdot\frac{1}{\eta_{50;0.6}} - 3\cdot\frac{1}{\eta_{100;0.6}} \tag{24}$$

Since the Schmidt-Sauer parameters v_{loss} and r_{loss} describe a situation with pure active power (meaning cos $\varphi = 1$), inserting them in (21) and (22) results in the calculation rules for $v_{loss,a}$ and $r_{loss,a}$ that are given in (25) and (26).

$$v_{loss,a} = v_{loss} - v_{loss,b} \tag{25}$$

$$r_{loss,a} = r_{loss} - r_{loss,b} \tag{26}$$

The LEM is fully characterized with these parameters. If the use of other measurement points is desired, it is necessary to adjust the calculation rules by setting up and solving the system of equations for these points.

In summary, when efficiency values for five operating points ($\eta_{10;1}$; $\eta_{50;1}$; $\eta_{90;1}$; $\eta_{50;0.6}$; $\eta_{100;0.6}$) are known, the model parameters can be determined with the calculation rules given in (4), (5), (6), (23), (24), (25), and (26). Any type of inverter will have an individual set of parameters (p_{self}; $v_{loss,a}$; $r_{loss,a}$; $v_{loss,b}$; $r_{loss,b}$) describing its efficiency plane versus apparent power and power factor. By inserting these parameters in (21), (22), and finally (20), inverter losses for any value of apparent power and any power factor can be predicted with the LEM.

VI. MODEL PARAMETRIZATION AND VALIDATION

Both models can be parametrized for a specific PV inverter by applying the calculation rules described in Sections IV and V. As shown before, the EEM requires nine independent points where conversion efficiency is measured, whereas five measurement points are needed to set up the LEM. In order to apply the calculation rules shown in Sections IV and V, it is important to perform the efficiency measurements at the specified exact operating points (P; Q) (see Fig. 5) respectively (S; cos φ) (see Fig. 8). For the present study, this could be ensured

by using interpolated values as described in Section III. For other measurement points, different equation systems need to be set up and solved.

For model validation, the EEM as well as the LEM were parametrized by using the interpolated efficiency values obtained for the specified operating points for all three inverters. Since for these inverters efficiency measurements at a wide range of measurement points were performed (see Section III), it is possible to assess the accuracy of the models by comparing the measured efficiencies with the modeled values at each point.

Fig. 10 and Fig. 11 show the parametrized efficiency models EEM and LEM (colored plains) for the 50 kVA inverter. The black dots represent all points that were taken for the measurements described in Section III.

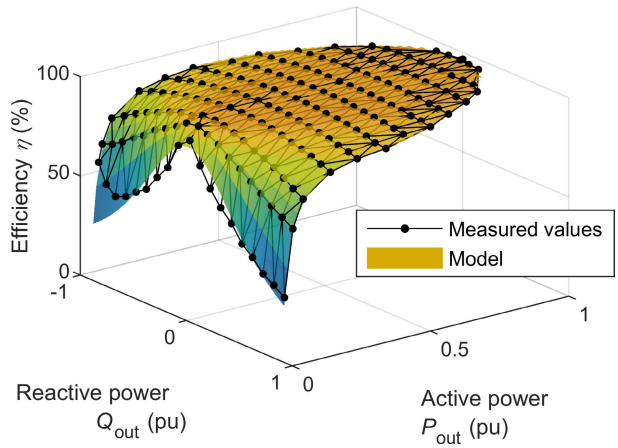

FIGURE 10. Results of the empirical efficiency model and measured efficiency values for the 50 kVA inverter.

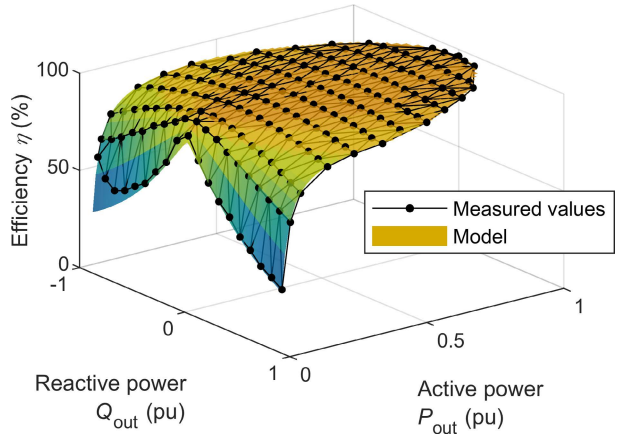

FIGURE 11. Results of the loss-based efficiency model and measured efficiency values for the 50 kVA inverter.

To validate the precision of the models, the average model error $\bar{\epsilon}$ as well as the standard deviation σ of the model error were calculated by comparing the measured efficiency η_{Meas} for every measurement point i with the modeled efficiency η_{Model} for the same working point, as shown in (27) and (28).

$$\bar{\epsilon} = \frac{\sum_{i=1}^{n} \left|\eta_{\text{Model,i}} - \eta_{\text{Meas,i}}\right|}{n} \tag{27}$$

$$\sigma = \sqrt{\frac{\sum_{i=1}^{n} \left(\left|\eta_{\text{Model,i}} - \eta_{\text{Meas,i}}\right| - \bar{\epsilon}\right)^2}{n-1}} \tag{28}$$

Table 1 lists the resulting average errors and the corresponding standard deviations for EEM and LEM for all three inverters. For comparison, the same values are shown for Braun's model that was parametrized by using the efficiency values ($\eta_{10;0}$; $\eta_{50;0}$; $\eta_{90;0}$) as suggested in [13]. Since current regulations typically require inverters to feed in reactive power for active power values greater than 0.1 pu only (see e.g. [29] and [30]), the values are specified separately for this operating area.

TABLE 1. Average error and standard deviation values for empirical efficiency model, loss-based efficiency model, and braun's model for all three inverters.

$\bar{\epsilon}$ / σ	EEM		LEM		Braun's model	
	full range	P > 0.1 pu	full range	P > 0.1 pu	full range	P > 0.1 pu
String inverter 36 kVA	**0.42%** ±1.14%	**0.08%** ± 0.14%	**0.87%** ±2.22%	**0.27%** ±0.45%	**0.65%** ±1.24%	**0.25%** ±0.25%
String inverter 50 kVA	**0.73%** ±1.58%	**0.09%** ±0.14%	**0.25%** ±0.55%	**0.05%** ±0.06%	**0.29%** ±0.59%	**0.05%** ±0.07%
Central inverter 1 MVA	**0.12%** ±0.20%	**0.06%** ±0.07%	**0.31%** ±0.58%	**0.21%** ±0.36%	**0.23%** ±0.28%	**0.17%** ±0.17%

Since different measurement points were used for each inverter, it is not possible to compare model errors between inverters. However, it is very well possible to compare the accuracy of the three models for each individual inverter. The smallest average errors for each inverter are highlighted in Table 1.

VII. MODEL SELECTION, APPLICABILITY AND LIMITATIONS

Table 1 shows that all three models result in average errors smaller than 1% for every inverter that was considered and for both the full operating range and the P > 0.1 pu area. This underlines the general applicability of the models, especially for grid studies where the overall losses of different reactive power provision methods are to be assessed. For PV park yield assessments, a high accuracy of the model is even more important since inverter losses are mirrored directly in a reduced performance ratio. For this application however, the errors for $P > 0.1$ pu are of greater interest, since reactive power provision is not required outside this operating range in practice. Average model errors are considerably smaller in this area, reaching less than 0.1% for all tested inverters with the EEM that seems particularly suitable for this operating

range. Moreover, the error distribution is rather narrow here, as is proven by the considerably smaller standard deviation of errors in this operating range.

Braun's model can be set up with known efficiency values for three measurement points only. All measurement points are allowed to have unity power factor. Despite this limited effort in setting up the model, it shows good accuracy for all three inverters that were considered in this study.

From a mathematical point of view, it can be said that the LEM is a generalization of Braun's model, where parameter functions $v_{\text{loss}}(\cos\varphi)$ and $r_{\text{loss}}(\cos\varphi)$ replace the constant parameter values of Braun's model. Because of this higher complexity of the LEM, it may lead to smaller error values than Braun's model for inverter types where the influence of the power factor on the losses is larger (e.g. for inverters where the conductivities of the switches and the diodes differ considerably, see Section V). For the three considered inverters, this is not consistently the case: Braun's model even results in smaller average errors for the 36 kVA and the 1 MVA inverters. This demonstrates that the choice of the measurement points that are used for parametrization has a considerable influence on model accuracy.

One limitation of both Braun's model and the LEM is that due to their mathematical structure, the calculated efficiency values for inductive and capacitive reactive power of the same magnitude are always identical. This implies a symmetrical nature of the relationship between reactive power provision and electrical losses. In reality, the reactive power consumption of the grid-side filter causes a deviation of the maximum efficiency values from the symmetry axis $Q = 0$. Among the devices considered in this study, this effect is greatest for the 36 kVA inverter. This is illustrated in Fig. 12 where three efficiency curves representing different active power values of the 36 kVA inverter are shown. It can be observed that maximum efficiencies are reached for reactive power values of approximately 0.07 pu for this inverter (green dots).

The EEM can replicate this effect. Therefore, its accuracy is not limited by the properties of the grid-side filter. For the

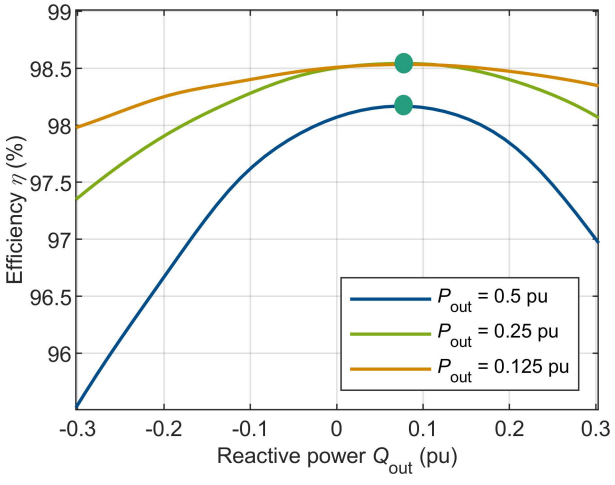

FIGURE 12. Efficiency curves of the 36 kVA inverter (interpolated measurement values) with marked peak efficiencies.

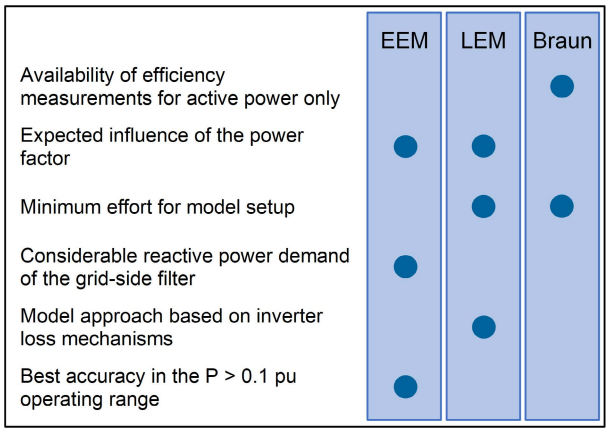

FIGURE 13. Possible criteria for model selection and description of distinctive model properties.

three considered inverters, its average error was the lowest of all models for the 36 kVA string inverter and the 1 MVA central inverter.

In conclusion, the selection of models can be based on several criteria depicted in Fig. 13, depending on the use case.

All three models primarily compute inverter losses, which can subsequently be used to calculate inverter efficiencies. Therefore, the models can still be employed if the electrical losses of an inverter are of greater interest than its efficiency. In particular, they can be used to assess the losses for operating points with very low active power values or even phase-shifting, i.e. situations when the concept of inverter efficiency loses its meaningfulness.

Both the EEM and the LEM were tested with three inverters of different power categories and topologies. The results were compared with the established model proposed by Braun. The applicability of the models for all three inverters and the relatively similar model accuracies hint to the general suitability of both new approaches for the efficiency modeling of inverters for active and reactive power provision. Moreover, the generic structure of the EEM and the underlying physical explanations of the internal loss mechanisms used in the LEM suggest a general applicability for many different inverter types.

Obviously, every model has its limitations. Relative inverter losses for small active power output ($P < 0.1$ pu) are generally higher, yet the models have the lowest accuracy for this area. In practice today, this operating area plays a minor role for energy yield as well as for reactive power provision, so this greater inaccuracy is less significant.

All models work under the assumption that the efficiency plane is continuous and there are no sudden jumps or kinks in the efficiency curves. While this is true for alle common stand-alone PV inverters commercially available today, it may not be the case for devices working with master-slave concepts or other methods that entail the switching on and off of hardware components for different load situations. Moreover, while the models can be used for single-stage and multi-stage inverters, they only provide accurate results

for one constant DC voltage level. If the DC voltage level (or, more accurately, the ratio between DC and AC voltage) varies, different model parameters must be found for each voltage level. For multi-stage inverters, the combined efficiency of the entire device can be calculated with the model for a specific DC voltage level.

Another important limitation is that for a correct parametrization of the models, it is important to control the intended operating points for each efficiency measurement with great accuracy, which is not always easy. If this cannot be ensured, it is possible to solve the resulting equation systems for any measurement points. Alternatively, as has been done in this study, interpolation methods can be used.

VIII. CONCLUSION

The main objective of this work was to investigate the conversion efficiency of PV inverters in different scenarios of active and reactive power generation. After measuring the efficiency of three inverters at several operating points, two new representation models were proposed. These models, the Empirical Efficiency Model and the Loss-Based Efficiency Model, can be used to predict the losses and thus the inverter efficiency over the entire operating range (P; Q). To determine the model parameters, the exact value of the efficiency must be known at nine (Empirical Efficiency Model) or five (Loss-Based Efficiency Model) operating points. In this paper, the derivation of the models as well as the calculation steps which are required for their parametrization are described.

For all three inverters, the efficiency values computed with the models were compared with a large set of measurement values. Both models achieve good accuracy and applicability for all three inverters. The average errors between efficiency values predicted with the models and the measured efficiencies were compared between the two new models and a preexisting one which is referred to as Braun's model. The Empirical Efficiency Model gives very low average error values, especially for active power values greater than 0.1 pu. The Loss-Based Efficiency Model is even less laborious to apply and gives high accuracy especially for inverters with a relatively small influence of the grid-side filter's reactive power consumption. It can be argued that it should be possible to use both models for many different inverter types with good accuracy: The Empirical Efficiency Model due to its generic approach, and the Loss-Based Efficiency Model because the general physical loss mechanisms of inverters were taken into account for its conception. They exceeded the accuracy of Braun's model in several situations and are designed to provide good accuracy even for inverters where losses are highly dependent on the power factor or not symmetrical to the zero reactive power axis.

The models enable a detailed forecast of the inverter losses for any operating point, allowing the determination of the cost of reactive power supply from PV inverters. This information can be used for grid studies where the overall cost of reactive power supply from different sources is to be compared, or for PV park operators who aim to assess the individual cost of reactive power provision of their assets.

Future works in this field could focus on the applicability of the proposed models for further PV inverters or for battery and wind turbine converters. Moreover, generic parameter sets for different classes of inverters could be identified, which would be particularly useful for grid studies. Another possible enhancement of the present efficiency models would be to integrate the dependency on the DC voltage. While this would probably cause a higher degree of model complexity, it would allow for an even more detailed description of the inverter efficiency in the varying operational conditions that PV inverters typically face.

REFERENCES

[1] J. W. Smith, W. Sunderman, R. Dugan, and B. Seal, "Smart inverter volt/var control functions for high penetration of PV on distribution systems," in *Proc. IEEE/PES Power Syst. Conf. Exposit.*, Phoenix, AZ, USA, Mar. 2011, pp. 1–6, doi: 10.1109/PSCE.2011.5772598.

[2] N. W. Miller and K. Clark, "Advanced controls enable wind plants to provide ancillary services," in *Proc. IEEE PES Gen. Meeting*, Minneapolis, MN, USA, Jul. 2010, pp. 1–6, doi: 10.1109/PES.2010.5589787.

[3] Y. Chistyakov, E. Kholodova, K. Netreba, A. Szabo, and M. Metzger, "Combined central and local control of reactive power in electrical grids with distributed generation," in *Proc. IEEE Int. Energy Conf. Exhib. (ENERGYCON)*, Florence, Italy, Sep. 2012, pp. 325–330, doi: 10.1109/EnergyCon.2012.6347775.

[4] H. Koppe, M. Schuster, B. Engel, and R. Grab, "Reactive power provision with distributed energy resources: Limitations, potentials and losses," in *Proc. IEEE Milan PowerTech*, Milan, Italy, Jun. 2019, pp. 1–6, doi: 10.1109/PTC.2019.8810550.

[5] *Datasheet SMA Sunny Tripower Core 2 STP 110–60*. SMA Solar Technology, Niestetal, Germany. Accessed: Feb. 17, 2022. [Online]. Available: https://files.sma.de/downloads/STP110-60-DS-en-14.pdf

[6] *Datasheet Enphase IQ 7 IQ 7+ Microinverters*. Enphase Energy, Fremont, CA, USA. Accessed: Feb. 17, 2022. [Online]. Available: https://enphase.com/sites/default/files/2021-04/IQ7-IQ7plus-DS-EN-U.S..pdf

[7] J. Jantsch, H. Schmidt, and J. Schmid, "Results of the concerted action on power conditioning and control," in *Proc. 11th Eur. Photovoltaic Solar Energy Conf. (PVSEC)*, Montreux, Switzerland, 1992, pp. 1589–1593.

[8] H. Schmidt and D. U. Sauer, "Practical modeling and estimation of inverter efficiencies," presented at the 9th Internationales Sonnenforum, Stuttgart, Germany, 1994, pp. 550–557.

[9] F. Baumgartner, H. Schmidt, B. Burger, H. Haeberlin, and M. Zehner, "Status and relevance of the DC voltage dependency of the inverter efficiency," in *Proc. 22nd Eur. Photovoltaic Sol. Energy Conf. Exhib. (PVSEC)*, Milan, Italy, 2007, pp. 2499–2505.

[10] R. Moghe, R. P. Kandula, A. Iyer, and D. Divan, "Losses in medium-voltage megawatt-rated direct AC/AC power electronics converters," *IEEE Trans. Power Electron.*, vol. 30, no. 7, pp. 3553–3562, Jul. 2015, doi: 10.1109/TPEL.2014.2350003.

[11] F. Gervasio, R. A. Mastromauro, and M. Liserre, "Power losses analysis of two-levels and three-levels PWM inverters handling reactive power," in *Proc. IEEE Int. Conf. Ind. Technol. (ICIT)*, Seville, Spain, Mar. 2015, pp. 1123–1128, doi: 10.1109/ICIT.2015.7125248.

[12] M. Braun, "Reactive power supplied by PV inverters—Cost-benefit analysis," in *Proc. 22nd Eur. Photovoltaic Sol. Energy Conf. Exhib.*, Milan, Italy, 2007, pp. 2940–2946.

[13] M. Braun, *Provision of Ancillary Services by Distributed Generators—Technological and Economic Perspective*. Kassel, Germany: Kassel Univ. Press, 2008, pp. 67–78.

[14] M. Farivar, R. Neal, C. Clarke, and S. Low, "Optimal inverter VAR control in distribution systems with high PV penetration," in *Proc. IEEE Power Energy Soc. Gen. Meeting*, San Diego, CA, USA, Jul. 2012, pp. 1–7, doi: 10.1109/PESGM.2012.6345736.

[15] X. Su, M. A. S. Masoum, and P. J. Wolfs, "Optimal PV inverter reactive power control and real power curtailment to improve performance of unbalanced four-wire LV distribution networks," *IEEE Trans. Sustain. Energy*, vol. 5, no. 3, pp. 967–977, Jul. 2014, doi: 10.1109/TSTE.2014.2313862.

[16] R. Grab, M. I. Rojas Flores, H. Schmidt, F. Hans, and S. Eichner, "Efficiency of inverters for reactive power feed-in," presented at the 35th PV-Symp., Bad Staffelstein, Germany, 2020, pp. 132–145.
[17] H. Laukamp, "Inverters for photovoltaic systems," presented at the Viertes Nationales Symp. Photovoltaische Solarenergie, Freiburg, Germany, 1989.
[18] *Overall Efficiency Grid Connected Photovoltaic Inverters*, Standard EN 50530, 2010.
[19] MathWorks. *Documentation MATLAB Pchip Function*. Accessed: Apr. 6, 2021. [Online]. Available: http://www.mathworks.com/help/MATLAB/ref/pchip.html
[20] MathWorks. *Documentation MATLAB Spline Function*. Accessed: Apr. 6, 2021. [Online]. Available: http://www.mathworks.com/help/MATLAB/ref/spline.html
[21] G. A. Rampinelli, A. Krenzinger, and F. Chenlo Romero, "Mathematical models for efficiency of inverters used in grid connected photovoltaic systems," *Renew. Sustain. Energy Rev.*, vol. 34, pp. 578–587, Jun. 2014, doi: 10.1016/j.rser.2014.03.047.
[22] A. Wintrich, U. Nicolai, W. Tursky, and T. Reimann, *Application Manual Power Semiconductors*. Ilmenau, Germany: ISLE Verlag, 2015, pp. 28–43.
[23] F. Blaabjerg, J. K. Pedersen, S. Sigurjonsson, and A. Elkjaer, "An extended model of power losses in hard-switched IGBT-inverters," in *Proc. IAS Conf. Rec. IEEE Ind. Appl. Conf. 31st IAS Annu. Meeting*, vol. 3, Oct. 1996, pp. 1454–1463, doi: 10.1109/IAS.1996.559258.
[24] F. Casanellas, "Losses in PWM inverters using IGBTs," *IEE Proc.-Electr. Power Appl.*, vol. 141, no. 5, pp. 235–239, Sep. 1994, doi: 10.1049/ip-epa:19941349.
[25] K. Berringer, J. Marvin, and P. Perruchoud, "Semiconductor power losses in AC inverters," in *Proc. IEEE Ind. Appl. Conf. 30th IAS Annu. Meeting*, vol. 1, Oct. 1995, pp. 882–888, doi: 10.1109/IAS.1995.530391.
[26] R. W. Erickson and D. Maksimovic, "Switch realization," in *Fundamentals of Power Electronics*, 2nd ed. Secaucus, NJ, USA: Kluwer Academic, 2007, pp. 92–96.
[27] J. Pinne, A. Gruber, K. Rigbers, E. Sawadski, and T. Napierala, "Optimization and comparison of two three-phase inverter topologies using analytical behavioural and loss models," in *Proc. IEEE Energy Convers. Congr. Exposit. (ECCE)*, Raleigh, NC, USA, Sep. 2012, pp. 4396–4403, doi: 10.1109/ECCE.2012.6342224.
[28] K. Venkatachalam, C. R. Sullivan, T. Abdallah, and H. Tacca, "Accurate prediction of ferrite core loss with nonsinusoidal waveforms using only Steinmetz parameters," in *Proc. 8th IEEE Workshop Comput. Power Electron.*, Mayaguez, PR, USA, Jun. 2002, pp. 36–41, doi: 10.1109/CIPE.2002.1196712.
[29] *Technical Connection Rules Medium Voltage*, Standard VDE-AR-N-4110, 2018.
[30] *Grid Connection of Energy Systems Via Inverters*, Standard AS/NZS 4777.2:2015, 2015.

ROBIN GRAB received the Diplom-Ingenieur degree in electrical engineering and information technology from the Karlsruhe Institute of Technology (KIT), Karlsruhe, Germany, in 2010. In 2010, he completed complementary studies in applied cultural sciences at KIT.

Since 2010, he has been with the Fraunhofer Institute for Solar Energy Systems, Freiburg, Germany. He leads a research team in the field of grid integration of inverter-based resources. Since 2017, he has been teaching photovoltaic systems technology at KIT.

FRANZISKA HANS received the B.S. degree in energy and environmental engineering from the Hamburg University of Technology, Germany, in 2016, and the M.S. degree in energy science and engineering from the Technical University of Darmstadt, Germany, in 2020.

Since 2021, she has been a Research Scientist with the Fraunhofer Institute for Solar Energy Systems, Freiburg, Germany. Her research interest includes the grid integration of renewable energies.

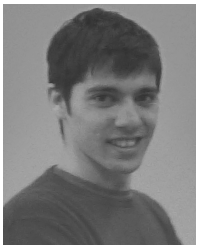

MARIANO IVAN ROJAS FLORES received the Graduate degree in electrical engineering from the National University of San Juan (UNSJ), San Juan, Argentina, in 2019.

In 2018, he was an Intern at the Fraunhofer Institute for Solar Energy Systems, Freiburg, Germany. He worked in the field of grid integration of inverter-based resources. From 2019 to 2021, he worked on electrical studies in power systems for the design of power plants and transformer substations. He currently works in the manufacturing of sucker rods at Techint S.A., San Luis, Argentina.

HERIBERT SCHMIDT was born in Cologne, Germany, in 1952. He received the M.S. degree and the Ph.D. degree in electrical engineering from the Technical University of Aachen (RWTH), Germany.

Since 1988, he has been with the Fraunhofer Institute for Solar Energy Systems ISE, where he did research work in the field of power electronics, holding more than 25 patents. In 2011, he received the Joseph-von-Fraunhofer price for the invention of the HERIC inverter topology. From 1985 to 2017, he gave lectures on photovoltaic systems technology at the Karlsruhe Institute of Technology (KIT), Karlsruhe, Germany. He is currently a Senior Engineer and a fellow of Fraunhofer ISE.

SOENKE ROGALLA received the Diplom-Ingenieur degree in electrical engineering and information technology from the Karlsruhe Institute of Technology (KIT), Karlsruhe, Germany, in 2006, and the Ph.D. degree in electrical engineering from the University of Braunschweig—Institute of Technology, Germany, in 2020.

Since 2006, he has been with the Fraunhofer Institute for Solar Energy Systems, Freiburg, Germany. He was responsible for different research groups in the fields of PV inverter development, high power electronics, inverter testing, PV system concepts, grid interaction of converters, and grid-forming converters. Since 2022, he has been the Co-Head of the Department Power Electronics and Grid Integration.

BERND ENGEL (Member, IEEE) was born in Gross-Gerau, Germany, in 1966. He received the Graduate degree from the Technical University of Darmstadt, Germany, in 1991, and the Ph.D. degree in electrical engineering from the Technical University of Clausthal, Germany, in 1996. From 1996 to 2003, he was with ALSTOM Transport Deutschland GmbH, Salzgitter, Germany. In 2003, he joined SMA Solar Technology AG, Kassel, Germany, to become the Senior Vice President for Technology and Product Development. Since 2011, he has been a University Professor at the Technical University of Braunschweig, Germany, where his main research focus is the components of sustainable energy systems. His research interests include the grid and market integration of renewables, batteries, electric mobility, and hydrogen components.